View metadata, citation and similar papers at core.ac.uk
brought to you by CORE
provided by CERN Document Server

Preprint typeset in JHEP style. - HYPER VERSION

CPTH-S726.0799
LPTENS-99/26
hep-th/9909171

High Energy Scattering on Distant Branes

C. Bachas

Laboratoire de Physique Théorique de l' Ecole Normale Supérieure[*]
24 rue Lhomond, F-75231 Paris Cedex 05, France
bachas@lpt.ens.fr

B. Pioline

Centre de Physique Théorique[†],
Ecole Polytechnique, F-91128 Palaiseau, France
pioline@cpht.polytechnique.fr

Abstract: We consider the elastic scattering of two open strings living on two D-branes separated by a distance r. We compute the high-energy behavior of the amplitude, to leading order in string coupling, as a function of the scattering angle ϕ and of the dimensionless parameter $v = r/(\pi\alpha'\sqrt{s})$ with $\sqrt{s}$ the center-of-mass energy. The result exhibits an interesting phase diagram in the (v, ϕ) plane, with a transition at the production threshold for stretched strings at $v = 1$. We also discuss some more general features of the open-string semiclassical world-sheets, and use T-duality to give a quantum tunneling interpretation of the exponential suppression at high-energy.

Keywords: D-branes, high-energy scattering, quantum tunneling.

[*]Unité mixte du CNRS et de l ENS, UMR 8549.
[†]Unité mixte du CNRS et de l' EP, UMR 7644

Contents

1. Introduction

The purpose of the present work is to discuss some aspects of the high-energy fixed-angle scattering of open strings. In string perturbation theory such scattering is exponentially soft and is dominated by smooth semiclassical trajectories [1, 2, 3, 4, 5]. From a technical viewpoint the external energy-momentum vectors can be thought of as null Minkowski charges on the worldsheet, and the saddle-point trajectories correspond to configurations of electrostatic equilibrium. Such configurations have been exhibited at each order in the genus expansion by Gross and Mende [3]. They describe the elastic scattering of two closed untwisted strings and also, after appropriate identifications [4, 5], of two open strings or of a single closed-string off a D-brane. The amplitude for all these fixed-angle processes decays exponentially fast with the squared center-of-mass energy (s) or momentum transfer (t). The suppression is, however, less and less severe at higher orders, so that perturbation theory will eventually break down [6]. This is consistent with the existence of some novel, possibly parton-like structure at substringy distances [7] (see also [8, 9, 10]).

An interesting variation of the saddle-point problem arises when the scattering strings are held a finite distance r apart. This can be the distance between two D-branes in the case of open strings, or between two orbifold fixed-points in the case of twisted closed strings. For open strings, the leading contribution to the scattering amplitude comes from worldsheets with cylindrical topology. The cylinder stretches between the two distinct D-branes which, in the 'electrostatic analog', behave like capacitor plates. Our main technical result in the present work will be the exact solution of this modified electrostatic problem, generalizing the result of [2, 4].

The relevant new parameter turns out to be $v = r/(\pi\alpha'\sqrt{s})$, in accordance with the naive expectation that the size of fundamental strings grows with the center-of-mass energy as $\sim \alpha'\sqrt{s}$. We will show that the amplitude has an interesting phase structure in the (v, ϕ) plane, where ϕ is the angle of scattering. As v ranges from infinity to zero at fixed ϕ, our solution interpolates continuously between massless closed-string exchange and the exponentially-soft behavior of [2, 4]. The electrostatic equilibrium becomes unstable at $v < 1$, reflecting the fact that we have crossed the threshold for production of two massive stretched strings at an intemediate state. This qualitative change of behavior may be of phenomenological relevance, particularly in the context

of low-string-scale models, in which the threshold $v = 1$ for nearby branes could be in the few-TeV region.

The exponential suppression of the perturbative high-energy amplitudes is reminiscent of a quantum tunneling process, and also of a minimal surface (soap-bubble) problem. T-duality in open-string theory makes these interpretations precise. Open string theory allows furthermore a better understanding of the relation between 'electrostatic stability' on the world sheet and unitarity cuts of the corresponding amplitude. These simple comments have not been discussed to our knowledge previously in the literature, and shed interesting new light on the physics of high-energy collisions. We have devoted a (non-technical) part of our paper to explaining them.

The plan of the paper is as follows: in section 2 we review the saddle-point calculation of the disk amplitude, with an emphasis on topological features of the semiclassical trajectory that generalize to higher orders. In sections 3 and 4 we set up and solve the saddle point problem on the annulus, and discuss the phase diagram of the amplitude in the (v, ϕ) plane. We end with some comments on T-dual interpretations of the high-energy collision process.

2. Topology of Semiclassical Trajectories

We consider the scattering of two incoming open-string states (1 and 2) into two outgoing open-string states (3 and 4), with Mandelstam variables $s = -(p_1 + p_2)^2$, $t = -(p_1 + p_3)^2$ and $u = -(p_1 + p_4)^2$. The high-energy fixed-angle behavior of the amplitude does not depend on the details of the external states, provided all masses are kept finite in the limit. We can assume thus for simplicity that all the external states are massless. In terms of the center-of-mass energy E and scattering angle ϕ the Mandelstam variables read

$$s = 4E^2 \ , \quad -ts = \sin^2\phi 2 \ , \quad \text{and} \quad -us = \cos^2\phi 2 \ , \tag{2.1}$$

where ϕ ranges from 0 for forward scattering to π for backward scattering. Note that in the physical kinematic region s is positive while t and u are negative. Momentum conservation implies that $s + t + u = 0$.

The high-energy behavior at tree-level can be extracted from the Veneziano formula,

$$\mathcal{A}_{\rm disk}^{(oo\to oo)} \sim \frac{\Gamma(-\alpha' t)\Gamma(-\alpha' u)}{\Gamma(\alpha' s)} + (s \leftrightarrow t) + (s \leftrightarrow u) \ . \tag{2.2}$$

The three terms in the above amplitude correspond to different topological arrangements of the external states, and are multiplied by the Chan-Paton factors tr(1324), tr(1234) and tr(1243) respectively. Using Stirling's approximation for the Gamma functions, $\Gamma(x) \sim \sqrt{2\pi} x^{x-1/2} e^{-x}$, one finds

$$\mathcal{A}_{\rm disk}^{(oo\to oo)} \sim e^{-\alpha' \tilde{\mathcal{E}}_{\rm disk}} \tag{2.3}$$

where the exponential weight is given by

$$\begin{aligned}\tilde{\mathcal{E}}_{\rm disk} &= s\log|s| + t\log|t| + u\log|u| \\ &= -s\left[\cos^2\phi 2\log\left(\cos^2\phi 2\right) + \sin^2\phi 2\log\left(\sin^2\phi 2\right)\right]\end{aligned} \tag{2.4}$$

Strictly-speaking only the first of the three terms in (2.2) has a well-behaved asymptotic limit in the physical kinematic region. The other two have a series of poles at integer values of $\alpha' s$, corresponding to the excited open strings that can propagate on-shell in the intermediate channel. For these singular amplitudes, the asymptotic limit refers to the residue at the poles, or to the imaginary (absorptive) part averaged over some range of incoming momenta. Note that the amplitude without s-channel poles is obtained when the incoming strings interact by joining and splitting in the middle,

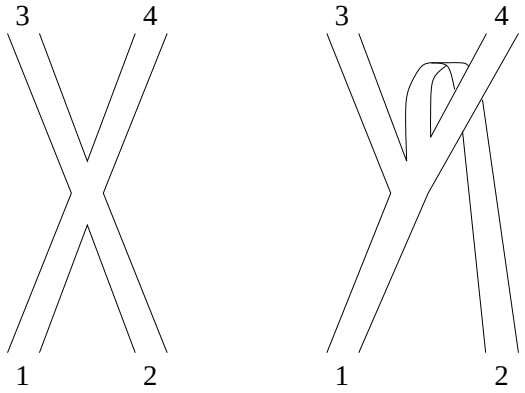

Figure 1: Open-string amplitudes with (left) or without (right) s-channel poles

as illustrated in figure 1. Note also that the asymptotic limit has forward/backward symmetry, as can be seen from the fact that $\phi \leftrightarrow \pi - \phi$. amounts to exchanging the Mandelstam variables t and u.

It is instructive to rederive the above results by a saddle point calculation, in which one extremizes the 'electrostatic energy' of four null Minkowski charges placed at the boundary of a disk. The advantage of the 'electrostatic' calculation is that it can be extended to more general situations when the amplitude – an integral over positions of the vertex operators and moduli of the world-sheet – does not admit a closed-form expression. Let us represent the disk as the upper-half plane, and let x_i be the points of insertion of the vertex operators on the boundary. The Veneziano amplitude is given by an integral

$$\mathcal{A}^{(oo\to oo)}_{\rm disk} \sim \int d\zeta\ e^{-\alpha'\mathcal{E}_{\rm disk}}\ , \tag{2.5}$$

where $\zeta = (x_1 - x_3)(x_2 - x_4)/(x_1 - x_2)(x_3 - x_4)$ is the $Sl(2,R)$ invariant cross-ratio, and the 'electrostatic energy' reads

$$\mathcal{E}_{\rm disk} = t\log|\zeta| + u\log|1-\zeta|\ . \tag{2.6}$$

If we use the $SL(2,R)$ symmetry to fix $x_1 = 0$, $x_2 = 1$ and $x_4 = \infty$, then $\zeta = x_3$. The (1324), (1234) and (1243) permutations of external states correspond therefore to the integration intervals $(0,1), (1,\infty)$ and $(-\infty, 0)$. The first of these three integrals is as expected real and convergent, while the other two diverge as $|\zeta| \to \infty$, and must be defined by analytic continuation.

The electrostatic energy $\mathcal{E}_{\rm disk}$ has a saddle point at

$$\tilde{\zeta} = -ts = \sin^2 \phi 2 \ , \tag{2.7}$$

where it takes precisely the value in (2.4). Since this is the only saddle point in the complex ζ-plane, we expect it to govern the behavior of the amplitude for any ordering of the external states. What is important, however, to realize is that the topology of the semiclassical trajectory is always of the (1324) type – $\tilde{\zeta}$ goes indeed from 0 to 1 as the scattering angle ranges from 0 to π. This is not of course surprising : a smooth semi-classical trajectory of the (1234) or (1243) type would have been incompatible with the fact that highly-excited open strings can propagate on-shell at an intermediate stage. In the language of the electrostatic analog, the two incoming particles 'attract' so that they cannot equilibriate if they are adjacent. Note furthermore that the configuration (2.4) is one of stable equilibrium, as should be expected of a saddle point which governs the behavior of an integral that is both real and convergent. [1]

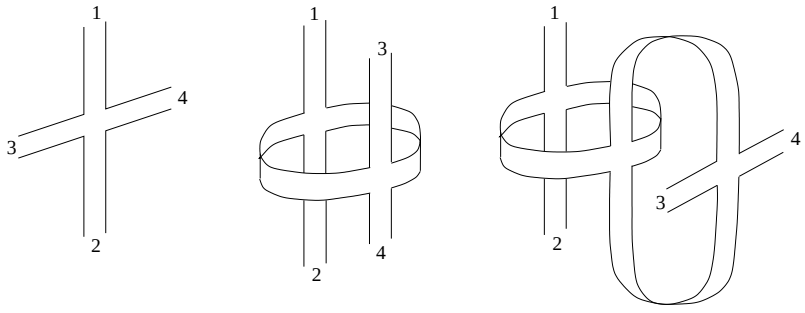

Figure 2: Topology of higher-genus saddle points

Extending these arguments to higher orders, leads us to expect that the saddle-point trajectories have a topology forbidding one-particle intermediate states to go on-shell. This can be achieved by insisting that successive scatterings are of the non-planar type shown in figure 1. Two such successive scatterings correspond, in particular, to the non-planar annulus diagram, three scatterings to the disk diagram with a closed-string handle etc (see figure 2). More generally for any odd (or even) number N of scatterings one finds a world-sheet topology with one (or two) boundaries and $[N-12]$ closed-string handles. That the relevant semi-classical trajectories should be of this type

[1] The equilibrium is on the other hand unstable if we allow the charges to move off the real axis. This reflects the fact that in closed-string amplitudes one cannot suppress the s-channel poles by a suitable choice of Chan-Paton factors.

agrees with the observation of Gross and Manes [4] that, in the corresponding electrostatic problem, empty world-sheet boundaries are 'shrunk away to zero by electrostatic pressure'.

3. Deformed Gross-Mende Saddle Points

The elastic scattering discussed in the previous section assumed massless open-strings living on a set of coincident D-branes. We want now to analyze what happens when the scattering strings live on two D-branes separated by a distance r. The kinematics of one such process is illustrated in figure 2. The two incoming open strings (1 and 2) live on two distant D-branes, as do the two outgoing strings (3 and 4). The amplitude, proportional to the Chan-Paton factor tr(13)tr(24), receives contributions from world-sheets with at least two boundaries, so that the leading perturbative contribution comes from the cylinder (or annulus) diagram. The topology of figure 2 is special in that it does not allow one-particle unitarity cuts. The (12)(34) topology, by contrast, has both open- and closed-string channel poles, the topologies with three insertions on a boundary have intermediate open-string poles, while the topologies with an empty boundary allow a massless closed-string to propagate at zero momentum down the throat. Following our discussion in the previous section, we should therefore expect the relevant semiclassical trajectories to have the (13)(24) or the (14)(23) topologies.

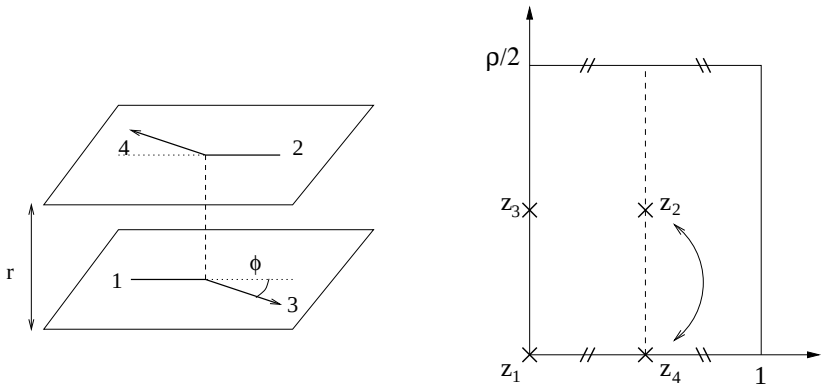

Figure 3: Kinematics and saddle point configurations on the annulus

Let us set up now the corresponding electrostatic problem. We consider the annulus as a (doubling) torus of modulus $\tau = i\rho/2$, modded out by a reflection symmetry along the imaginary axis. The bosonic propagator for fields on the boundaries reads

$$G(z|\tau) = \log\chi \ , \quad \chi = 2\pi e^{-\pi y^2/\tau_2}\Big|\theta_1(z|\tau)\theta_1'(0|\tau)\Big| \ , \tag{3.1}$$

where $z = x + iy$ and $\theta_1' = 2\pi\eta^3$. Using the momentum conservation and mass-shell

conditions one finds the following expression for the 'electrostatic energy'

$$\begin{aligned}\mathcal{E}_{\rm annulus} = r^2\rho 4\pi{\alpha'}^2 &+ s\left[\log|\theta_1(z_{12})\theta_1(z_{34})| - 2\pi(y_{12}^2+y_{34}^2)/\rho\right]\\ &+ t\left[\log|\theta_1(z_{13})\theta_1(z_{24})| - 2\pi(y_{13}^2+y_{24}^2)/\rho\right]\\ &+ u\left[\log|\theta_1(z_{14})\theta_1(z_{23})| - 2\pi(y_{14}^2+y_{23}^2)/\rho\right]\end{aligned} \tag{3.2}$$

Here the ρ-dependence of the Jacobi functions has been suppressed, and $z_{ij} = z_i - z_j$ is the relative position of the inserted vertex operators, which obeys $\mathrm{Re} z_{ij} = 0, 1/2$ for i, j lying on the same or opposite boundaries. The amplitude is given by an integral over the positions z_i of the 'charges' and over the modulus ρ of the world-sheet,

$$\mathcal{A}_{\rm annulus}^{(oo\to oo)} \sim \int d\rho \prod_i \oint dz_i \, e^{-\alpha'\mathcal{E}_{\rm annulus}} \ . \tag{3.3}$$

The novel feature in expression (3.2) is the contribution to the 'electrostatic energy' due to the stretching of the world-sheet between the two branes. It can be thought of as the energy of a constant field created by a fixed potential drop between the two boundaries of the surface. A simple scaling argument shows that the relevant new parameter is

$$v = r\pi\alpha'\sqrt{s} \ . \tag{3.4}$$

This can be interpreted as the (inverse) ratio of the effective size of the incoming strings, which grows as $\sim \alpha'\sqrt{s}$ at high energies, to the distance r between the branes. Alternatively, it is the mass of a pair of strings that stretch between the two D-branes, divided by the total center-of-mass energy. The significance of these facts will become apparent in the following section.

The saddle points of $\mathcal{E}_{\rm annulus}$ are harder to analyze than those of $\mathcal{E}_{\rm disk}$. Following refs. [3, 4] we focus our attention to configurations in which the four charges are placed half-a-cycle apart on the doubling torus. Symmetry ensures that the energy is then automatically extremized under variations of the z_i. There are two such configurations with the topology (13)(24),

$$\begin{aligned}&\text{(A)}: \quad \tilde{z}_1 = 0 \ , \quad \tilde{z}_2 = 12 + i\rho 4 \ , \quad \tilde{z}_3 = i\rho 4 \ , \quad \tilde{z}_4 = 12 \ ,\\ &\text{and}\\ &\text{(B)}: \quad \tilde{z}_1 = 0 \ , \quad \tilde{z}_2 = 12 \ , \quad \tilde{z}_3 = i\rho 4 \ , \quad \tilde{z}_4 = 12 + i\rho 4 \ ,\end{aligned} \tag{3.5}$$

(see figure 3). Using standard properties of the Jacobi θ functions we find the following electrostatic energies for them:

$$\mathcal{E}^{(A)} = r^2\rho 4\pi{\alpha'}^2 + 2s\log|\theta_3| + 2t\log|\theta_4| + 2u\log|\theta_2| \ , \tag{3.6}$$

and

$$\mathcal{E}^{(B)} = r^2\rho 4\pi{\alpha'}^2 + 2s\log|\theta_2| + 2t\log|\theta_4| + 2u\log|\theta_3| \ , \tag{3.7}$$

where the θ-functions are evaluated at zero argument. The problem is now reduced to that of finding extrema of these energies with respect to the surface modulus $\tau = i\rho/2$.

We will here solve this mathematical problem analytically – the physical implications of our results will be discussed in the following section. It will be enough to analyze configuration (A), since for (B) we need only interchange the roles of s and u in our final expressions. Extremizing the energy (3.6) with respect to ρ gives the equation

$$r^2 8\pi\alpha'^2 + s\theta_3'\theta_3 + t\theta_4'\theta_4 + u\theta_2'\theta_2 = 0 \tag{3.8}$$

where $\theta_j' \equiv \partial_\rho \theta_j = i2\partial_\tau \theta_j$. Let us first recall how this equation is solved in the case of coincident branes [4]. The trick is to identify the Mandelstam variables with the three terms of the Riemann identity $\theta_3^4 - \theta_4^4 - \theta_2^4 = 0$. It is indeed straightforward to check that the ansatz

$$s = a{\theta_3}^4 \ , \quad t = -a{\theta_4}^4 \ , \quad u = -a{\theta_2}^4 \ . \tag{3.9}$$

solves both the constraint $s + t + u = 0$, and the saddle-point equation when $r = 0$. The saddle-point modulus $\tilde{\tau} = i\tilde{\rho}/2$ is, in this special case, determined implicitly by the Picard map,

$$-us = \cos^2\phi 2 = \left(\theta_2(\tilde{\tau})\theta_3(\tilde{\tau})\right)^4 \ , \tag{3.10}$$

which is one-to-one from the fundamental domain for the modular group $\Gamma(2)$ to the complex plane. The modulus $\tilde{\tau}$ is hence a function of the scattering angle only, as expected. The energy at the saddle point takes the value

$$2\tilde{\mathcal{E}}^{(A)}\Big|_{v=0} = s\log|s| + t\log|t| + u\log|u| \tag{3.11}$$

$$= -s\left[\cos^2\phi 2\log(\cos^2\phi 2) + \sin^2\phi 2\log(\sin^2\phi 2)\right] \ , \tag{3.12}$$

which is exactly half the electrostatic energy on the disk, in agreement with the one-loop result of Gross and Manes [4]. Intuitively the exponential suppression is less severe because the total momentum transfer is split between two equally-softer scatterings. Note incidentally that, at fixed collision energy, the maximal suppression is attained at right-angle scattering and corresponds to a square semiclassical world-sheet ($\tilde{\tau} = i$).

Extending the above trick to non-zero r requires a modular identity whose three terms add up to a non-vanishing constant. Such an identity, well known from the study of BPS saturated string amplitudes, is

$$\left[\theta_3^2\theta_3'\theta_3' - \theta_4^2\theta_4'\theta_4' - \theta_2^2\theta_2'\theta_2'\right]/\eta^{12} = -\pi^2 4 \ . \tag{3.13}$$

Using this and the second derivative of the Riemann identity it can be checked that

$$s = a{\theta_3}^4 + b\theta_3'\theta_3^3\eta^{12} \ , \quad -t = a{\theta_4}^4 + b\theta_4'\theta_4^3\eta^{12} \ , \quad -u = a{\theta_2}^4 + b\theta_2'\theta_2^3\eta^{12} \ , \tag{3.14}$$

solves the constraint and the saddle-point problem (3.8) provided one chooses

$$b = r^2 2\pi^3 \alpha'^2 \equiv \frac{sv^2}{2\pi} \ . \tag{3.15}$$

It will be useful to recast the above solution in a form that expresses the saddle-point modulus $\tilde{\rho}$ as a function of v and of the scattering angle ϕ. Eliminating a gives the implicit relation

$$-us = \cos^2\phi 2 = (\theta_2\theta_3)^4 \times \left[1 + \theta_3^4 v^2 2\pi\eta^{12}\left(\theta_2'\theta_2 - \theta_3'\theta_3\right)\right] \ . \tag{3.16}$$

This can be further simplified with the help of the identities :

$$\theta_2'\theta_2 = -\pi 24\left(E_2 + \theta_3^4 + \theta_4^4\right) \tag{3.17a}$$

$$\theta_3'\theta_3 = -\pi 24\left(E_2 + \theta_2^4 - \theta_4^4\right) \tag{3.17b}$$

$$\theta_4'\theta_4 = -\pi 24\left(E_2 - \theta_2^4 - \theta_3^4\right) \tag{3.17c}$$

where $E_2 = -(24/\pi)\partial_\rho \log\eta$ is the holomorphic weight-2 Eisenstein series. Some straightforward algebra leads to the following relation between $\bar{\rho}$, v and ϕ,

$$\text{(A)} \ : \quad -us = \cos^2\phi 2 = \theta_2^4(\bar{\tau}) - v^2\theta_3^4(\bar{\tau}) \ . \tag{3.18}$$

This generalizes the Picard map (3.10) to the case of non-coincident branes. For later convenience we write explicitly also the relation obtained for the configuration in which positions z_2 and z_4 have been exchanged. Exchanging s and u (and remembering that s entered also in the definition of v) we find

$$\text{(B)} \ : \quad -us = \cos^2\phi 2 = \theta_3^4(\bar{\tau}) - v^2\theta_2^4(\bar{\tau}) \ . \tag{3.19}$$

As will be verified numerically in the coming section, these equations give *all* the extrema of $\mathcal{E}^{(A)}$ and $\mathcal{E}^{(B)}$ on the real positive ρ-axis. We will also see that depending on the values of ϕ and v, eq. (3.19) has one, two or zero real solutions – in the latter case this means that our formal ansatz was inconsistent.

We close this section with some remarks on other possible saddle points. First, in addition to A and B, there are four more configurations of electrostatic equilibrium, at fixed ρ, corresponding to inequivalent permutations of the charges. The extrema $\tilde{\rho}$ of their energy must satisfy an equation obtained from (3.18) after an appropriate permutation of the Mandelstam variables. The (14)(23) extrema are in fact the same as A and B, up to an exchange of ϕ with $\pi - \phi$. For the (12)(34) configurations, on the other hand, the ρ-extremization has no solution, because the attracting pairs of charges tend to shrink the boundaries of the annulus to a point. The corresponding amplitude must be obtained by deforming the z_i integration contours, as was the case for the resonnant amplitudes at disk-level. A harder question concerns saddle points in the complex τ-plane, which become as we will see relevant in kinematic regions where the (13)(24) amplitude must be analytically continued. For $v = 0$, all saddle points are modular transform of one another, and yield the same energy as A. For $v > 0$ however, modular invariance is broken and the degeneracy between these saddle points is lifted.

4. Phase Diagram of the Amplitude

We now want to use the above results in order to evaluate the amplitude for the scattering process (13)(24) in the asymptotic high-energy limit. To this end let us first consider the potential singularities of the integral (3.3). Its three possible degeneration limits,

$$(a)\ \ z_{13} \text{ or } z_{24} \to 0\ ,\ \ (b)\ \ \rho \to 0\ ,\ \ \text{and}\ \ (c)\ \ \rho \to \infty\ , \tag{4.1}$$

correspond to an intermediate (a) open string, (b) closed string, or (c) pair of stretched strings going on shell. We have already argued that the first two singularities are absent because the momentum flowing out of a boundary is space-like. It can be indeed verified immediately that the electrostatic energy (3.2) goes to $+\infty$ in the limit (a), as long as the momentum transfer t stays negative. To analyze the other limits one should note that, at fixed ρ, configuration B is a global minimum of the energy. This is because the attracting (repelling) charges are as close (as far) from each other as they could be. We need therefore only check whether the energy of this configuration stays bounded from below as ρ varies. Using the asymptotic properties of θ functions, and the definition (3.4) of the parameter v, we find :

$$\mathcal{E}^{(B)} \overset{\rho\to 0}{\sim} -\frac{\pi t}{\rho} + 2t\log 2 + \frac{\pi v s}{4}\rho + \cdots \tag{4.2}$$

$$\mathcal{E}^{(B)} \overset{\rho\to\infty}{\sim} \frac{\pi s}{4}(v-1)\,\rho + 2s\log 2 + \cdots\ , \tag{4.3}$$

where the dots denote exponentially-small corrections. The limit (b) is thus energetically forbidden, as expected, while in the limit (c) the energy stays bounded from below if and only if $v > 1$. The reason for this is easy to understand : $v = 1$ is the critical separation at which the available center-of-mass energy suffices to create a pair of open strings stretching between the two branes. The instability of the electrostatic problem for $v < 1$ signals therefore the opening of a two-particle production threshold, and the appearance of an imaginary part to the amplitude.

Since, for $v > 1$, the integral (3.3) is real and convergent, it must be dominated by the minimum 'electrostatic energy' in the integration range, i.e. by $\mathcal{E}^{(B)}(\tilde{\rho})$ at $\tilde{\rho}$ given implicitly by (3.19). We have solved this equation numerically, and have plotted the results in figure 4. Note first that the solution to the equation is unique, and that it corresponds indeed to a global minimum. The two interesting limits to consider are (i) the limit of large brane separation ($v \to \infty$) and (ii) the approach to the stretched-string production threshold ($v \to 1_+$). In the $v \to \infty$ limit, the saddle point approaches zero as $\tilde{\rho} \sim 2\pi\alpha'\sqrt{-t}/r$. and the amplitude takes the asymptotic form

$$\mathcal{A}^{(oo\to oo)}_{\text{annulus}} \overset{v\to\infty}{\sim} e^{-r\sqrt{-t}-2t\alpha'\log 2}\ . \tag{4.4}$$

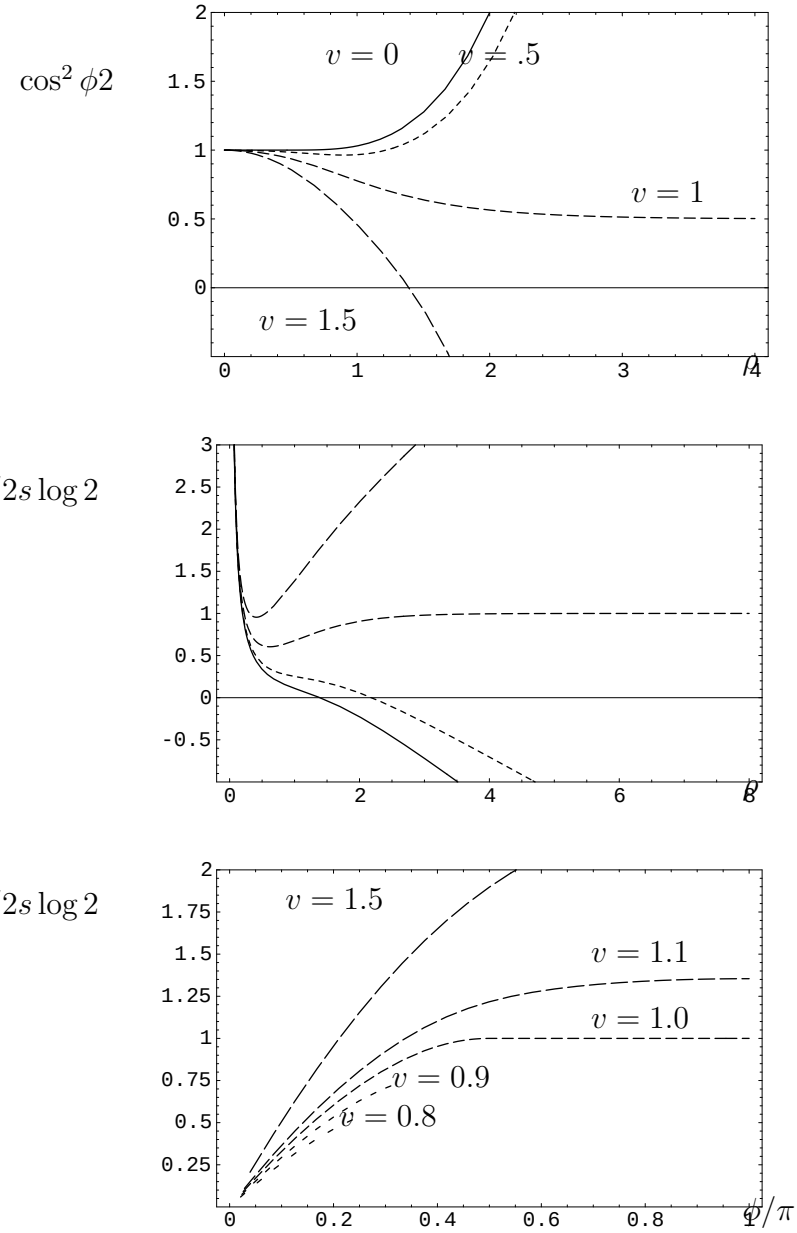

Figure 4: Deformed saddle point B. Top: $\cos^2\phi 2$ vs. modular parameter ρ as in (3.19). Middle: electrostatic energy vs. modular parameter ρ at small scattering angle $\phi = \pi/10$. Bottom: electrostatic energy at the minimum vs. angle. The solid line corresponds to coincident branes, and the dashed lines to separated branes .

The leading exponential behavior is characteristic of the exchange of massless closed-string modes between the branes,

$$e^{-r\sqrt{t}} \sim \int d\vec{p}\, e^{-i\vec{p}\,\vec{r}}\vec{p}^{\,2} + t \ , \tag{4.5}$$

with $\vec{p}$ the transverse momentum of the closed string, which is not conserved at each individual vertex. The subleading term in the exponential is more intriguing. A simple calculation shows that it cannnot be accounted for by the exponentially-rising density of intermediate states – it represents thus an effective exponential enhancement (since

t is positive) of the off-shell vertices. Consider next the $v \to 1_+$ limit. The imaginary (absorptive) part of the amplitude is easy to calculate at threshold, because the two stretched strings are in their ground state and at rest. We will see in the following section that the production of two large unexcited stretched strings at rest in a collision is a process T-dual to elastic right-angle scattering. This implies that

$$\mathrm{Im}\mathcal{A}^{(oo\to oo)}_{\text{annulus}} \overset{v\to 1_-}{\sim} \left|\mathcal{A}^{(oo\to oo)}_{\text{disk}}(\pi/2)\right|^2 \sim e^{-2s\alpha' \log 2} \ . \tag{4.6}$$

Let us compare this to the electrostatic energy plotted for $v = 1_+$ in figure 4. As ϕ goes from 0 to $\pi/2$ the minimum of the energy rises from 0 to $2s \log 2$, where it stays frozen while the angle of scattering continues to vary between $\pi/2$ and π. Thus the absorptive part saturates the amplitude for backward scattering, while it is subleading when compared to the real part for forward scattering. The semiclassical trajectory for backward scattering becomes singular ($\tilde{\rho} \to \infty$) at the threshold as expected.

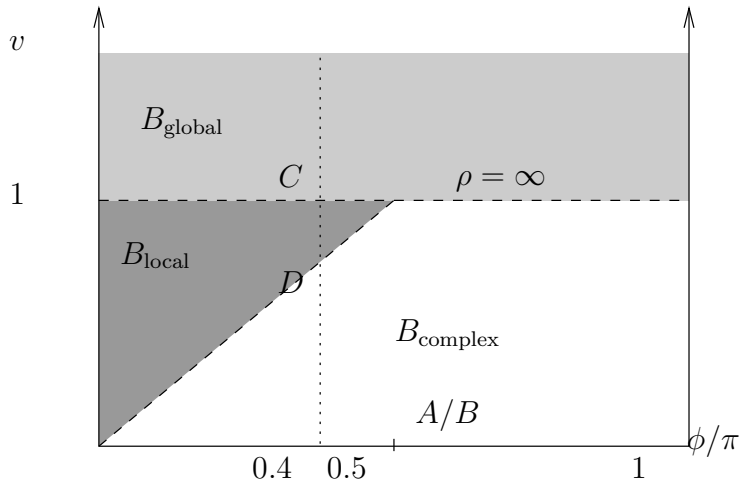

Figure 5: Phase diagram of the dominant saddle point. The saddle point is a global or local minimum of energy in the two shaded regions. The slice at $\phi = 2\pi/5$ is shown in figure 6 as an illustration.

We next turn to the region $v < 1$. Since $\mathcal{E}^{(B)}(\rho)$ goes from $-\infty$ to ∞, it must now have an even number of extrema. What we have found numerically are two distinct regions, separated by a boundary which goes from the point $(\pi/2, 1)$ to the origin in the (ϕ, v) plane (see figure 5). In the left region $\mathcal{E}^{(B)}(\rho)$ has two extrema – a local minimum and a local maximum, depicted as B and B' in figure 6 – which, by continuity, should govern the behavior of the real and of the imaginary parts of the amplitude. In this region the absorptive part continues to be exponentially smaller than the real part. As v approaches 1 from below, the local maximum saturates the imaginary part of the amplitude (point C in figure 6), as the corresponding world-sheet modulus runs away to infinity. The local minimum on the other hand crosses smoothly the $v = 1$ threshold, ensuring a continuous real part of the amplitude. At the phase boundary the two saddle points coalesce (point D in figure 6), before moving off the imaginary

τ-axis. In the right region, $\mathcal{E}^{(B)}(\rho)$ has thus no real saddle point at $v < 1$, and the amplitude must be governed either by the complex solutions of (3.19), or else by the configuration A.

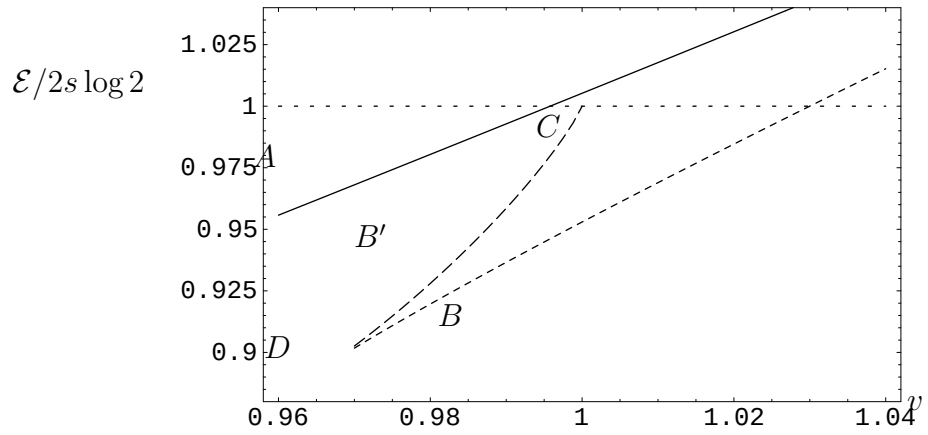

Figure 6: Energy of the deformed saddle points A and B as a function of the distance v for scattering angle $\phi = 2\pi/5$. A exists at all values of v, whereas B starts appearing at a critical value $v_D(\phi)$ as a pair of local minima and maxima B and B'. The latter disappears at $v = 1$ (C), while the former extends smoothly to $v > 1$. At $v < v_D$, B and B' move off the imaginary τ line.

In order to clarify this issue we now turn to an analysis of the saddle-point configuration A. In contrast to configuration B which is one of stable equilibrium on a given surface, this configuration is unstable under displacements of the positions z_i, due to the proximity of repelling charges. An asymptotic analysis, on the other hand, shows that $\mathcal{E}^{(A)}(\rho)$ has a minimum $\tilde{\rho}$ for all possible (v, ϕ). We find numerically that this minimum is unique, and ranges from 0 to a finite value when v is increased from zero to infinity, in contrast to the $v = 0$ case where ρ runs away to infinity as the angle approaches π (see figure 7). In particular, the solution experiences no discontinuity at the $v = 1$ threshold .

If configuration A is the dominant saddle-point when $v = 0$, we may expect it to remain dominant throughout the lower right region of figure 5. Our numerical investigation of the solution shows, however, that this is impossible. The energy $\tilde{\mathcal{E}}^{(A)}$ at the phase boundary is larger than the energy $\tilde{\mathcal{E}}^{(B)}$ (see figure 6), implying an unacceptable exponential jump in the amplitude. Such an exponential discontinuity is, in particular, incompatible with our calculation of the absorptive part (4.6) near threshold. Thus the dominant saddle point in this region should be the complex saddle-point of type B. As v goes to zero, the latter goes over to a modular transform of the saddle point A, consistently with the hypothesis of [4] that A dominates the amplitude when $v = 0$.

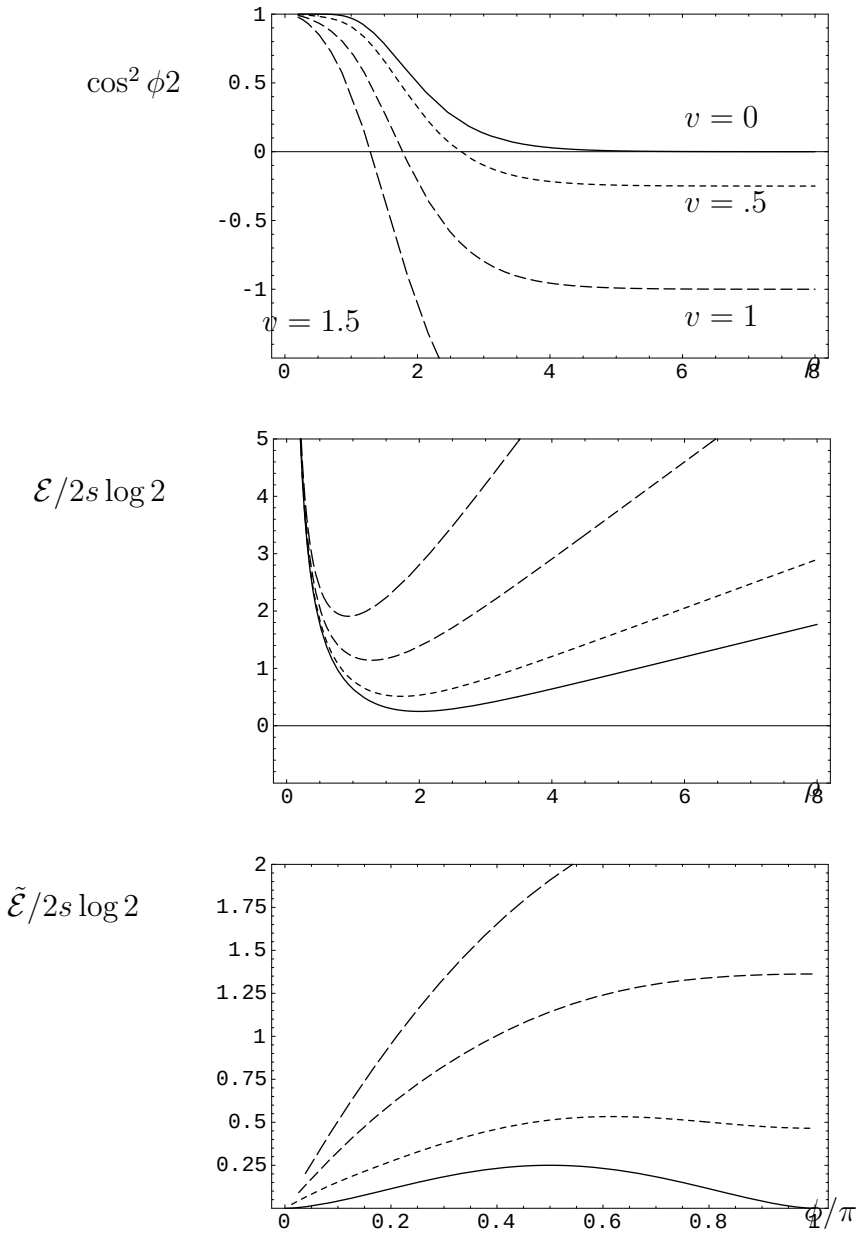

Figure 7: Deformed saddle point A. Top: $\cos^2\phi 2$ vs. modular parameter ρ as in (3.18). Middle: electrostatic energy vs. modular parameter ρ at right-angle scattering. Bottom: electrostatic energy vs angle. The solid line corresponds to coincident branes, and the dashed lines to separated branes.

5. Minimal Surfaces and Quantum Tunneling

The exponential behavior of the amplitudes is suggestive (a) of quantum tunneling, and (b) of a minimal-area problem. In this section we will use T-duality to render these two statements explicit. Though the mathematics do not change, T-dual language renders as often several aspects of the physics more transparent. The key point is that under T-duality the fastly-moving open strings can turn into very long static strings stretched between far-separated D-branes.

Consider in particular a kinematical configuration T-dual to right-angle scattering, obtained by dualizing the direction of outgoing momenta. This amounts to keeping $p_1 = (E, p, 0), p_2 = (E, -p, 0)$ while replacing p_3 and p_4 by the T-dual light-like momenta $w_3 = (-E, 0, r/2\pi\alpha'),\ w_4 = (-E, 0, -r/2\pi\alpha')$, characterizing a pair of static unexcited strings stretching with opposite orientations between two D-branes. The Veneziano amplitude corresponds now to the amplitude for the production of these static strings in the collision of two fastly-moving massless quanta. The exponential behavior of the amplitude confirms the expectation that such processes should be suppressed by the small overlap of wavefunctions. This interpretation can be used to reproduce the absorptive part of the one-loop amplitude of section 4.

Another configuration T-dual to right-angle scattering, can be obtained by dualizing all four external momenta to $w_1 = (E, r/2\pi\alpha', 0),\ w_2 = (E, -r/2\pi\alpha', 0),\ w_3 = (-E, 0, r/2\pi\alpha'),\ w_4 = (-E, 0, -r/2\pi\alpha')$. The Veneziano amplitude is now interpreted as the amplitude for two oppositely oriented such strings to join and flip as depicted in figure 8. This transition requires pulling the two stretched strings so that they join in the middle, and can then separate in the perpendicular direction. The energy barrier due to the string tension, $(\sqrt{2}-1)r/\pi\alpha'$, is very large in the semiclassical regime under consideration, so that the tunneling is exponentially suppressed. The world-sheet instanton mediating this process corresponds to the minimal surface interpolating between the world-sheets of the strings 1 and 2 in the far past and those of 3 and 4 in the far future, and can be thought of as a 'soap-bubble' problem for a wire with the contour shown by the thick line on the left-hand side of figure 8. Deforming the square into a rhombus of angle ϕ corresponds to going away from the right-angle scattering point.

The saddle point analysis of high energy scattering actually tells us what is the precise minimal surface for this soap-bubble problem. Indeed, for a disk topology, the saddle point semi-classical configuration is given by [3, 4]

$$X^\mu_{\rm saddle}(z) = i\alpha' \sum_{i=1}^{4} w_i^\mu \left(\log(z - x_i) \pm \log(\bar{z} - x_i)\right) \tag{5.1}$$

where the $\pm$ sign corresponds to the Neumann or Dirichlet components respectively. Choosing the insertion points as $0, 1, 1/2, \infty$ as implied by (2.7) for right-angle scatter-

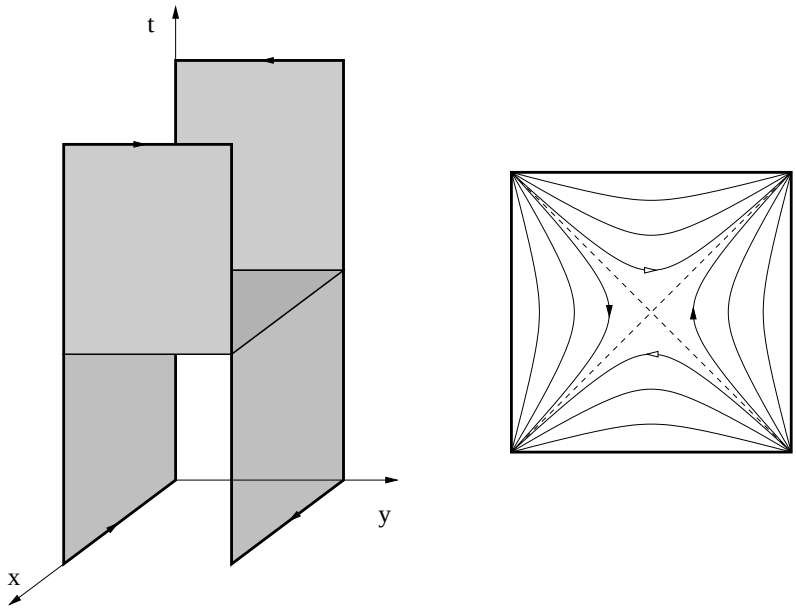

Figure 8: Disk-level high energy scattering in T-dual description. Left: two very long open strings of opposite orientation stretched between two pairs of D-branes undergo a flip transition. The heavy line defines the boundary for the corresponding soap-bubble problem. Right: time slices of the flip transition. The dark (resp. light) arrows represent the strings before (resp. after) the flip.

ing, gives

$$X^0(z,\bar{z}) = ir2\pi \log z\bar{z}(1-z)(1-\bar{z})(z-1/2)(\bar{z}-1/2) \tag{5.2a}$$

$$X^1(z,\bar{z}) = ir2\pi \log z(1-\bar{z})\bar{z}(1-z) \tag{5.2b}$$

$$X^2(z,\bar{z}) = ir2\pi \log z - 1/2\bar{z} - 1/2 \tag{5.2c}$$

It is easy to check that this solution satisfies the appropriate limits, for instance $X^0 \to -i\infty,\ X^1 \to r\theta/\pi,\ X^2 \to 0$ as $z \to 0$, where $\theta \in [0,\pi]$ depends on the direction in which $z = 0$ is approached. The area of the minimal surface is given by the saddle point energy $\alpha' s \log 2$ – this is smaller in particular than $\pi\alpha' s/2$ which corresponds to the instantaneous transition of figure 8. In fact, as emphasized in [3], higher genus world-sheets yield electrostatic energies which are a fraction of the above; this implies that the area of the film in the soap-bubble problem can be reduced by creating handles. In a realistic setting this is counterbalanced by a cost due to the extra curvature which prevents the surface from degenerating into a foam.

In string theory, the dominance of higher genus world-sheets implies that perturbation theory breaks down at high energy, unless the string coupling g_s controlling the curvature cost is tuned to zero at the same time as the energy is increased [6]. In particular, the contribution of D-instantons should be taken into account, and may drastically modify the exponential softness of the amplitude. High-energy scattering in the background of a D-instanton is known in particular to be power-suppressed [9],

implying that it is not a tunelling process. This is evident in our T-dual picture, since a D-instanton T-dualizes into an Euclidean D-brane cutting through figure 8 at a given time. The open string end-points can move freely on this slice, so that there is no energetic barrier to the flip transition.

Acknowledgments

The authors are grateful to the organizers of the Extended Workshop on String Theory at ICTP, Trieste, during which this work was started, for their kind hospitality and support. We also thank Eric D'Hoker, Michael Green and Elias Kiritsis for discussions. This research is supported in part by the EEC under the TMR contract ERBFMRX-CT96-0090.

Note added in proof. After the present work was completed, another work [11] appeared which discusses some related issues in the context of brane-world models, where quark and leptons are localized on separated walls. Their treatment is purely field-theoretical, and gives thus the characteristic $e^{-\sqrt{-t}r}$ behavior that we have discussed in section 4. Such a field-theoretical treatment would be applicable if the string scale were much heavier than the (Standard Model) Kaluza-Klein scale, which does not occur in weakly-coupled type I models (see however [12] for such a model in type IIB theory).

References

[1] G. Veneziano, *Nuovo Cim.* **57A** (1968) 190.

[2] V. Alessandrini, D. Amati and B. Morel, *Nuovo Cim.* **7A** (1971) 797.

[3] D.J. Gross and P.F. Mende, *Phys. Lett.***B197** (1987) 129; *Nucl. Phys.* **B303** (1988) 407.

[4] D.J. Gross and J.L. Manes, *Nucl. Phys.* **B326** (1989) 73.

[5] J.L.F. Barbon, *Phys. Lett.* **B382** (1996) 60, hep-th/9601098.

[6] P.F. Mende and H. Ooguri, *Nucl. Phys.* **B339** (1990) 641.

[7] S. Shenker, hep-th/9509132; T. Banks, W. Fischler, S. H. Shenker and L. Susskind, *Phys.Rev.* **D55** (1997) 5112, `hep-th/9610043`.

[8] M. Douglas, D. Kabat, P. Pouliot and S. Shenker, Nucl.Phys. **B485** (1997) 85 , hep-th/9608024 ; C. Bachas, *Phys.Lett.* **B374** (1996) 37, hep-th/9511043; D. Kabat and P. Pouliot, *Phys.Rev.Lett.* **77** (1996) 1004, hep-th/9603127; U. Danielsson, G. Ferretti and B. Sundborg, *Int.J.Mod.Phys.* **A11** (1996) 5463, hep-th/9603081.

[9] M.B. Green and M. Gutperle, *Nucl. Phys.* **B498** (1997) 195, hep-th/9701093; M.B. Green, *Nucl. Phys.* **B124** (1977) 461.

[10] S. Giddings, F. Hacquebord and H. Verlinde, *Nucl. Phys.* **B537** (1999) 260, hep-th/9804121; T. Wynter, hep-th/9905087.

[11] N. Arkani-Hamed, Y. Grossman and M. Schmalz, hep-ph/9909411.

[12] I. Antoniadis and B. Pioline, Nucl. Phys. **B550**, 41 (1999), hep-th/9902055